Conference Proceedings

Solar World Congress 2015
Daegu, Korea, 08 – 12 November 2015

# Heat conductivity performance of SiC and $Si_3N_4$ as volumetric receiver under concentrated irradiation

**M. Nakakura[1], M. Ohtake[1], T. Yoshida[1], K. Matsubara[2], T. Kodama[1], K. Yoshida[3]**

[1] Faculty of Engineering, Niigata University, Ikarashi 2-nocho 8050, Nishi-ku, Niigata 950-2181, Japan

[2] Faculty of Engineering, Niigata University: Professor, Doctor of Engineering, Ikarashi 2-nocho 8050, Nishi-ku, Niigata 950-2181, Japan

[3] Institute of Applied Energy: Counselor, Doctor of Engineering, 1-14-2, Nishi-Shimbashi 1-Chome, Tokyo 105-0003, Japan

## Abstract

Recently, researchers of Niigata University and the Institute of Applied Energy (IAE) developed an air receiver-evaluation system equipped with 30$kW_{th}$ point-concentration simulator to support solar-thermal usage in middle to high temperature. 147mm×147mm×100mm monolithic silicon carbide (SiC) honeycomb block used as volumetric receiver sample, and some experimental results were gathered from demonstration tests. Also, its three-dimensional simulation method was developed on FLUENT 14.5, in parallel. This simulation, based on dual-cell approach, considers that thermal non-equilibrium between solid and fluid domains in porous region defined as volumetric receiver material. And, its calculation regions include the upper and lower air domains in the porous region; therefore, this method is able to analyze the influence of inlet/outlet air flow. Under the same condition with tests, power on aperture (POA) and air-mass flow rate (AMF), some numerical results indicated similar results. This paper describes an example compared simulation and computational result. Also, a comparison between receiver outlet air temperature and solid/fluid max temperature caused by receiver material (SiC and $Si_3N_4$: silicon nitride) is presented.

Keywords: *CSP, Volumetric receiver, Receiver evaluation, Three-dimensional simulation, Receiver material*

## 1. Introduction

At present, solar thermal assessment have been carried out by many institutes and researchers, for renewable and clean solar thermal usage attract attention as an alternative energy to fossil fuels (Tsoutsos et al., 2003; Reif and Alhalabi, 2015). In Europe and United States, parabolic-trough solar plants are in operation to produce electricity to grid through the commercial operating. But its ability of electricity production is not enough for energy demand grown larger every year. On the other hands, tower type Concentrated Solar Power (CSP) plant is possible to achieve higher temperature than traditional solar plant because of its high concentrating ratio; therefore, there is a possibility of making a high efficiency generation (Ávila-Marín, 2011). A tower CSP plant combined with traditional Combined Cycle (CC), also called Solar-driven Combined Cycle (SCC), for practical solar-thermal utilization is expected to solve the energy problem people face today (Poživil et al., 2014). In order to realize the SCC technology, there are some studies of volumetric receiver using porosity material (mesh, foam, or honeycomb etc.) and its material (metal or ceramics etc.) (Fend et al., 2004; Ávila-Marín et al., 2014; Sallaberry et al., 2015). But, these research are still on fundamental stage and a lot of information (e. g. receiver geometry, material and thermal property etc.) are necessary to design high-temperature and -durability receiver.

In 2013, researchers of Niigata University and IAE developed an air receiver-evaluation system used a world-class 30$kW_{th}$ beam-down point concentration sun simulator and its three-dimensional simulation method for


doi:10.18086/swc.2015.04.07 Available at http://proceedings.ises.org

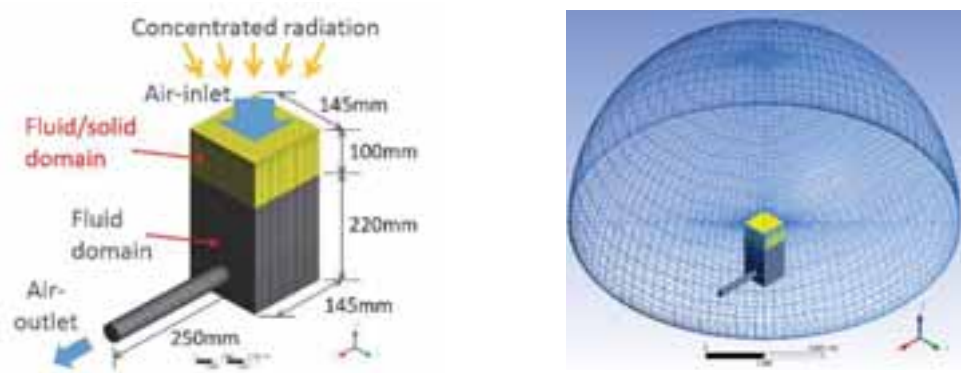


(a) The mesh of volumetric receiver (b) The calculation domain

**Fig. 1 The three-dimensional simulation model.**

research and development of solar-thermal receivers in middle to high temperature range (Nakakura et al., 2015). This evaluation system is possible to test by a beam-down point concentration, independent of unstable natural environment. Also, its simulation based on the dual-cell approach considers that thermal non-equilibrium between fluid and solid domain. Its numerical model includes upper/lower fluid domain on receiver; accordingly the influence of inlet-/outlet-air on receiver is able to analyze in detail. In this paper, the receivers of SiC and $Si_3N_4$ are simulated to reveal their suitability as volumetric receiver material.

## 2. Calculation model and boundary conditions

The computational model of the volumetric receiver flow and heat transfer was developed on ANSYS FLUENT 14.5. Figure 1 shows the mesh model of volumetric receiver and its calculation domain. Receiver material domain defines that porous medium have a solid domain within fluid one, and its size is similar to experimental sample 145mm×145mm×100mm. In this simulation, this porous domain is assumed to be a honeycomb geometry adapting the drag coefficient of rectangular to air flow direction. This three-dimensional simulation based on the dual-cell approach considers that the thermal non-equilibrium between the solid and fluid domain of the porous. Also heat flux distribution performed linear interpolation is adapted to the porous-surface as a boundary condition. This flux distribution was measured using Niigata University's 30$kW_{th}$ sun simulator through the scanning of a gardon gage (Nakakura et al., 2015). The outlet plane is used to definite air-mass flow rate (AMF), and the boundary of each plane is insulated. This calculation domain include upper and lower domain of the porous as a feature, hence this method is able to analyze the influence of inlet-/outlet-air flow effected to the porous medium.

The continuity and momentum equations are expressed as:

$$\nabla \cdot (\gamma \rho \vec{v}) = 0 \; ; \qquad \text{(eq. 1)}$$

$$\nabla \cdot (\gamma \rho \vec{v} \vec{v}) = \; -\gamma \nabla \rho + \nabla \cdot \mu \gamma (\nabla \vec{v} + \nabla \vec{v}^T) + \gamma \vec{B}_f - \left( \frac{\gamma^2 \mu}{K} \vec{v} + \frac{\gamma^3 C_2}{2} \rho |\vec{v}| \vec{v} \right). \qquad \text{(eq. 2)}$$

This momentum equation is added by the pressure loss term arising from the viscosity and inertia in the porous domain. In this equation, γ represents porosity, $B_f$ is body force, 1/K is viscous loss coefficient, and $C_2$ is inertial loss coefficient. This model assumes incompressible ideal gas, and considers the temperature dependency of density, viscosity and specific heat. Also SST k-ω model is used as turbulence equation; it follows,

$$\frac{\partial}{\partial x_i}(\rho k u_i) = \frac{\partial}{\partial x_j}\left( \Gamma_k \frac{\partial k}{\partial x_j} \right) + G_k - Y_k \;\; , \qquad \text{(eq. 3)}$$

$$\frac{\partial}{\partial x_i}(\rho \omega u_i) = \frac{\partial}{\partial x_j}\left( \Gamma_\omega \frac{\partial \omega}{\partial x_j} \right) + G_\omega - Y_\omega + D_\omega \; . \qquad \text{(eq. 4)}$$

In this instance, Γ is effective diffusivity, Y is dissipation due to turbulence, G is generation term, and $D_\omega$ is cross-diffusion term. The subscript k represents turbulence kinetic energy, and ω represents specific

**Tab. 1: The calculation parameters.**

| Elements | Porosity γ | Material | Density $\rho_s$ (kg $m^{-3}$) | Thermal conductivity $k_s$ ($Wm^{-1}K^{-1}$) | Specific heat $C_{ps}$ (J $kg^{-1}$ $K^{-1}$) | |
|---|---|---|---|---|---|---|
| 179202 | 0.538 | SiC | 3200 | 90 | 1000 | |
| | | Si3N4 | 3300 | 27 | 650 | |
| Specific surface $A_{fs}$ ($m^{-1}$) | Heat transfer coefficient at radiated surface $h_{fs}$ (W $m^{-2}$ $K^{-1}$) | Ambient air temperature $T_{amb}$ (K) | Viscos loss coefficient 1/K[X, Y, Z] | Inertial loss coefficient $C_2$[X, Y, Z] | Apparent absorptivity $\alpha_{app}$ | Apparent emissivity $\varepsilon_{app}$ |
| 2105 | 114.2 | 300 | 0, 0, 0 | 100, 100, 0.432 | 0.70, 0.83 | 0.70, 0.83 |

dissipation rate. Energy equations based on the dual-cell approach can be written as:

$$\frac{\partial}{\partial t}\left(\gamma\rho_f E_f\right) + \nabla\cdot\left(\vec{v}\left(\rho_f E_f + p\right)\right) = \nabla\cdot\left(\gamma k_f \nabla T_f - \left(\sum_i h_i J_i\right) + \left(\bar{\bar{\tau}}\cdot\vec{v}\right)\right) + h_{fs}A_{fs}\left(T_s - T_f\right) \quad \text{(eq. 5)}$$

$$\frac{\partial}{\partial t}\left((1-\gamma)\rho_s E_s\right) = \nabla\cdot\left((1-\gamma)k_s\nabla T_s\right) + h_{fs}A_{fs}\left(T_f - T_s\right). \quad \text{(eq. 6)}$$

The dual-cell approach solves each energy equation for fluid/solid domains, under thermal non-equilibrium assumption; so it takes into consideration of the interaction of heat transfer, in porous domain. Each energy equation of solid/fluid domain is added non-equilibrium source. In these energy equations, E refers to total energy, k is thermal conductivity, and $h_{fs}$ is heat transfer coefficient at radiated surface, $A_{fs}$ is specific surface. The subscript f represents fluid domain, s represents solid domain. Also, surface-radiation is treated as a boundary condition without using radiation models, described as:

$$Q_{total} = \alpha_{app}Q_{solar} + Q_{rad} \quad \text{(eq. 7)}$$

$$Q_{rad} = \sigma\varepsilon_{app}\left({T_{amb}}^4 - {T_{surf}}^4\right) \quad \text{(eq. 8)}$$

In this equation, $Q_{solar}$ refers to heat flux distribution adapted to porous surface, $\alpha_{app}$ and $\varepsilon_{app}$ are apparent absorptivity and emissivity due to receiver geometry, σ is Stefan-Boltzmann constant, $T_{amb}$ is ambient air temperature, and $T_{surf}$ is porous surface temperature. Table 1 summarizes numerical parameters used in this simulation.

## 3. Simulation results and analysis

### *3.1. Results of three-dimensional simulation*

Figure 2 indicates that a comparison between experimental results and simulation ones. The y-axis shows ΔT or efficiency, and the x-axis is POA/AMF. The ΔT is calculated from difference between the outlet air temperature and the ambient air temperature. Also, the efficiency represents the ratio of thermal absorption on an exhaust bulk air temperature to power-on-aperture (POA). Firstly, through some calculations under the same condition with the test, the numerical analysis is able to obtain the similar results with experimental ones in both of ΔT and efficiency. Hence, this simulation method indicates the accuracy of simulation as volumetric receiver evaluation. The difference of ΔT in the high-temperature range is estimated by temperature-independence on the porous media. Also, in the experimental tests, efficiency is calculated from heat-absorption of coolant water and exhaust air to POA; therefore, the value calculated from experimental results is lower than simulation results because there is a heat-conduction loss from air to water.

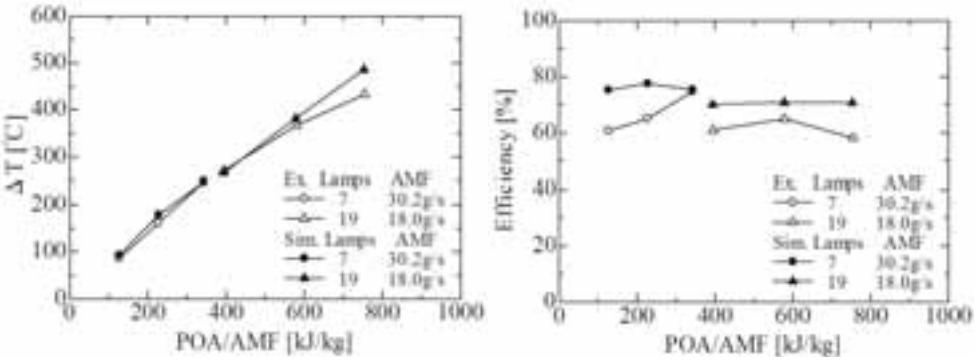


**(a) Delta T** **(b) Efficiency**

**Fig. 2 Comparison between experimental results and simulation ones.**

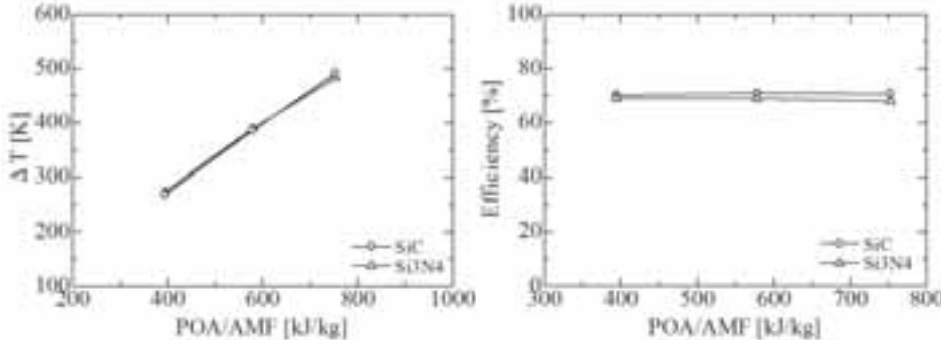


**(a) Delta T** **(b) Efficiency**

**Fig. 3 Comparison between SiC and $Si_3N_4$.**

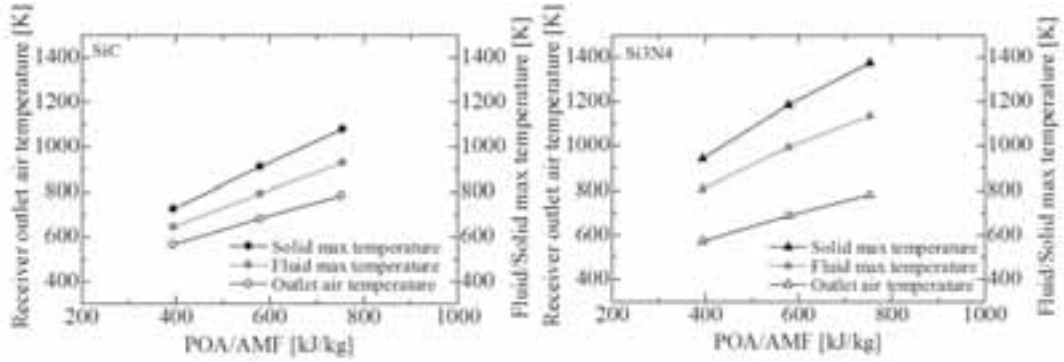


**(a) SiC** **(b) $Si_3N_4$**

**Fig. 4 Outlet air temperature and solid/fluid maximum temperature.**

Figure 3 designates results of ΔT and efficiency from some calculation fed the physical property of SiC or $Si_3N_4$. There are no significant difference both of ΔT and efficiency on the values. Approximately, ΔT is 500K, and efficiency is 70% both of cases.

Figure 4 shows a comparison of the outlet air-temperature and the solid/fluid maximum temperature in SiC or $Si_3N_4$. The outlet air-temperature, as shown in Fig. 3, don't reveal a difference between SiC and $Si_3N_4$. However, there are large gap on the solid and fluid maximum temperature. In relation to the solid maximum temperature, $Si_3N_4$ derives 1375K, and SiC shows 1061K. The difference in temperature between the solid max- and outlet air-temperature is 592K and 270K, in each case. Also, on the fluid maximum temperature, $Si_3N_4$ is 1134K, and SiC is 932K. The difference in temperature between the fluid max- and outlet air-temperature shows 351K and 141K, in each case. This cause of the differences between $Si_3N_4$ and SiC will be

discussed in detail, below.

### *3.2. Analysis of contours*

SiC and $Si_3N_4$ as a volumetric receiver material will be discussed from some counters of results acquired in subsection 3.1. All of the following figures are obtained from a state of POA/AMF=800kJ/kg.

Figure 5 indicates that fluid-temperature distribution on Z-X cross-section of the calculation model. The ambient air is heated on porous domain, and exhausted through the outlet pipe at approximately 800K. In the case of $Si_3N_4$, high temperature air reach down to more deep position than SiC. Also, the highest temperature appears into the slightly downward spot, not on the irradiated surface in both cases. These results are guessed from influence of inlet air-flow.

Similarly, figure 6 shows solid-temperature distribution on Z-X cross-section of the simulation model. There is the radial heat conductivity from irradiated centre in both cases. In the deep position of $Si_3N_4$, solid-temperature is higher than SiC, likewise the fluid-temperature. Also, slightly, solid-temperature at end of the porous media is lower; therefore large temperature distribution is able to be confirmed than SiC.

Figure 7 represents temperature distribution of porous surface. The thermal conductivity and specific heat of $Si_3N_4$ are lower than SiC. Hence, it is easy to increase temperature of irradiated point, but it is hard to expand the heat around the porous media.

Figure 8 shows a streamline of SiC. About a streamline, there was no noticeable difference between SiC and $Si_3N_4$. This simulation is possible to verify the behaviour of air-flow on the volumetric receiver from the upper and lower calculation domain. The ambient air is inhaled into the porous from extensive area, and accelerated at the outlet pipe.

By these counters, the solid maximum temperature of $Si_3N_4$ is approximately 300K higher, and, according to the low conductivity, temperature distribution is tend to be larger than SiC; therefore, only in the point of heat transfer performance, SiC is speculated the advantage as volumetric receiver material than $Si_3N_4$.

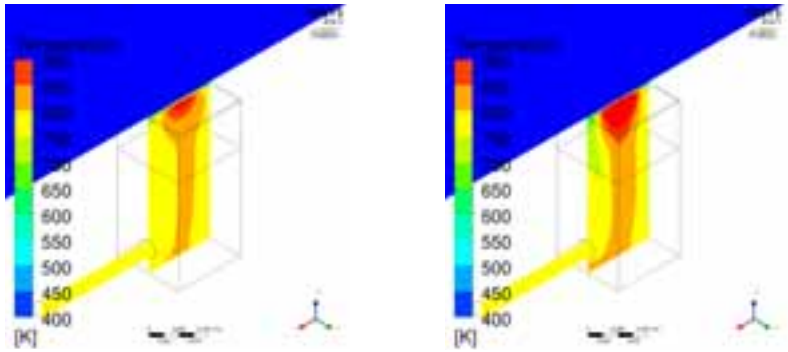


**(a) SiC** **(b) $Si_3N_4$**

**Fig. 5 Fluid temperature distribution on Z-X cross-section.**

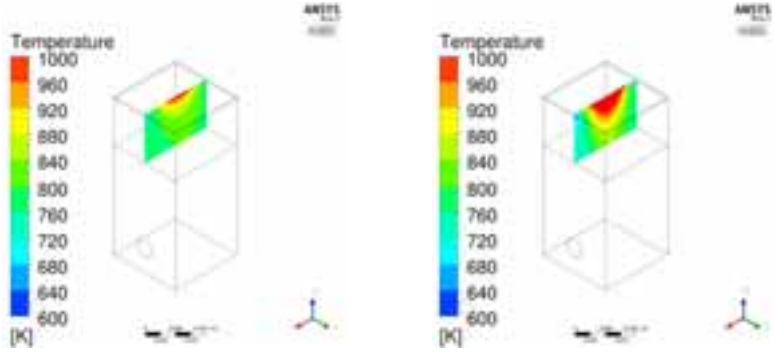


**(a) SiC** **(b) $Si_3N_4$**

**Fig. 6 Solid temperature distribution on Z-X cross-section.**

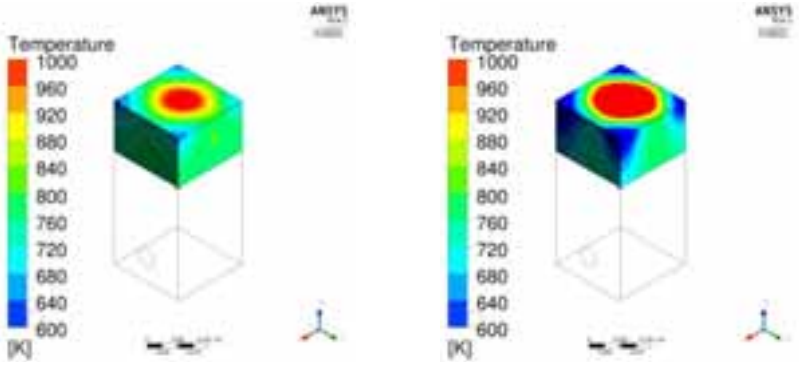


**(a) SiC** **(b) $Si_3N_4$**

**Fig. 7 Temperature distribution of porous surface.**

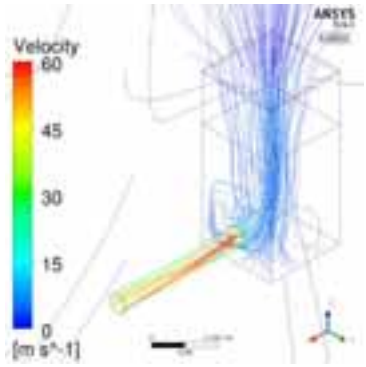


**Fig. 8 Streamline.**

## 4. Conclusion

(1) Niigata University and the Institute of Applied Energy developed a volumetric receiver evaluation system using world-class 30kW$_{th}$ point-concentration sun simulator and its three-dimensional simulation method.
(2) The accuracy as a simulation method was confirmed by the comparison between experimental- and numerical-results; therefore this method is able to be used in data acquisition related to the volumetric receiver or new design one.
(3) Under the same condition of POA and AMF, there was not much of a difference in the outlet air-temperature between SiC and $Si_3N_4$. Nevertheless, on the porous media, SiC possessed a small temperature distribution comparatively, hence the advantage of SiC as volumetric receiver was verified in the point of heat transfer ability.

## 5. References

Avila-Marin, A.L., 2011. Volumetric receivers in Solar Thermal Power Plants with Central Receiver System technology: A review. Sol. Energy 85, 891-910.
Avila-Marin, A.L., Alvarez-Lara, M., Fernandez-Reche, J., 2014. Experimental results of gradual porosity wire mesh absorber for volumetric receivers. Energy Procedia 49, 275-283.
Fend, T., Pitz-Paal, R., Reutter, O., Bauer, J., Hoffschmidt, B., 2004. Two novel high-porosity materials as volumetric receivers for concentrated solar radiation. Sol. Energy Mater. Sol. Cells 84, 291-304.
Nakakura, M., Ohtake, M., Matsubara, K., Yoshida, K., Cho, H.S., Kodama, T., Gokon, N., 2015. Development of a receiver evaluation system using 30 kWth point concentration solar simulator. Energy Procedia 69, 497-505.
Poživil, P., Aga, V., Zagorskiy, A., Steinfeld, A., 2014. A pressureized air receiver for solar-driven gas turbines. Energy Procedia 49, 498-503.

Reif, J.H., Alhalabi, W., 2015. Solar-thermal powered desalination: Its significant challenges and potential. Renew. Sustain. Energy Rev. 48, 152-165.
Sallaberry, F., García de Jalón, A., Zaversky, F., Vázquez, A.J., López-Delgado, A., Tamayo, A., Mazo, M.A., 2015. Towards standard testing materials for high temperature solar receivers. Energy Procedia 69, 532-542.
Tsoutsos, T., Gekas, V., Marketaki, K., 2003. Technical and economical evaluation of solar thermal power generation. Renew. Energ. 28, 873-886.